Comparison of dynamic response and levelized cost of energy on three platform concepts of floating offshore wind turbine systems

Comparison of dynamic response and levelized cost of energy on three platform concepts of floating offshore wind turbine systems

Yuka Kikuchi, Takeshi Ishihara

Department of Civil Engineering, The University of Tokyo, Hongo 7-3-1, Bunkyo-ku, Tokyo, JAPAN
kikuchi@bridge.t.u-tokyo.ac.jp

Abstract Spar, semisubmersible and barge platforms are modelled based on the full-scale demonstration projects in Japan for a generic 5 MW turbine. Three platforms are evaluated with the structural and stability parameters. The characteristic of floater motions and mooring forces are clarified by performing the dynamic analysis. The dynamic responses are validated with the water tank tests. The levelized cost of energy is assessed by using the engineering cost model.

1. Introduction

The floating offshore wind turbine system is promising in the deep-sea area. A wide range of floating platform concepts have been demonstrated in Norway, Portugal and Japan for floating offshore wind turbine (FOWT) systems. Spar concepts using gravity in the form of ballast are used in Hywind [1] and GOTO FOWT projects [2]. Semisubmersible concepts using distributed buoyancy are used in WindFloat [3] and Fukushima FORWARD projects [4]. In 2018, a barge platform using buoyancy from the large water plane area was installed to aim the cost reduction in the Next-generation offshore floating wind energy project [5]. Carbon Trust [6] summarized the recent demonstration projects and Taboada [7] reviewed different type of floating offshore wind foundations.

Butterfield et al. [8], [9] proposed the qualitative stability triangle and gave the qualitative assessment of spar, barge and TLP. These platforms were classified in terms of how they achieve basic static stability in the pitch and roll directions. These platforms provide restoring moments primarily through the mooring system combined with the excess buoyancy in the platform, a deep draft combined with the ballast and a shallow draft combined with the water plane area, respectively. Semisubmersible platform is a hybrid concept, which use restoring features from these three concepts. Jonkman and Matha [10] numerically investigated the ultimate loads on the towers of TLP, spar and barge concepts in 2011. It was found that the platform motion induced ultimate and fatigue loads for all turbine components in the barge system were the highest. The difference in the ultimate and fatigue loads between the MIT/NREL TLP system and OC3-Hywind system were not significant. Koo et al. [11] and Goupee et al. [12] experimentally compared the spar and semisubmersible platforms in 2014. Bagbanci et al. [13] numerically investigated dynamic responses of spar and semisubmersible concepts in 2015. The surge, heave and pitch amplitudes for the spar and semisubmersible platforms were observed to have a similar pattern as compared using both FAST code and water tank tests in Roddier et al. [14]. The levelized cost of energy for different platforms is also useful information. Myer et al. [15] investigated the levelized cost of energy for spar, TLP and semisubmersible by using

engineering cost model. However, the quantitative comparison between spar, semisubmersible and barge platforms has not been conducted yet.

In this study, spar, semisubmersible and barge platforms are modeled based on the full-scale demonstration projects conducted in Japan. The platform concepts are quantitatively evaluated with the structural and stability parameters. The dynamic responses are then investigated by the dynamic analysis and validated with the experimental data from the water tank tests. Finally, the levelized cost of energy for these three platforms are assessed by using the engineering cost model.

2. Static characteristics of three platform concepts

2.1. Model description

NREL 5 MW from the National Renewable Energy Laboratory [16] is used for the turbine model. The diameters and thickness of the tower bottoms are enlarged for the larger bending moments due to the floater motions. The hub heights are set as higher than the rotor diameters and are the same for all three platforms. Table 1 shows the principal dimensions and mass properties of NREL 5 MW wind turbine.

Three platforms are built based on the demonstration projects conducted in Japan. Figure 1 shows the overview of three platforms. The spar is modelled based on GOTO FOWT demonstration project and is scaled up from a 2MW turbine to a 5 MW turbine. The semisubmersible platform is based on Fukushima Floating Offshore demonstration project and also is scaled up from a 2MW turbine to a 5 MW turbine. The barge is built based on Next-Generation Floating Offshore project and is scaled up from 3 MW to a 5 MW turbine.

The principal dimensions and mass properties for each platform are shown in Table 2. The spar has a long draft and a small water plane. The barge has a short draft and a large water plane. Semisubmersible has a middle value between spar and barge. As a result, the displacement volume of water for the semisubmersible platform is the largest. Those for the spar and barge platforms are 61 % and 70 % of semisubmersible one as shown in Table 2. Figure 2 shows comparison of water plane are, draft and displacement of three platforms.

Table 1. Principal dimensions and mass properties of turbine.

Item	Unit	Designations
Power	MW	5.0
Blade mass	kg	17,740
Blade length	m	61.5
Hub mass	kg	56,780
Nacelle mass	kg	240,000
Tower top mass	kg	350,000
Tower mass	kg	514,000
Rotor diameter	m	126.0
Tower top diameter	m	3.78
Hub height	m	83.1

Table 2. Principal dimensions and mass properties for each platform.

Item	Unit	Spar	Semisubmersible	Barge
Height	m	130	32	11
Maximum width	m	9.4	67.5	51
Draft	m	120	21.3	7
Water plane area	m^2	67	691	1296
Displacement volume of water	m^3	8,029	13,084	9,123
Weight turbine and platform	ton	7,852	12,988	8,912
Platform weight including ballast	ton	6,988	12,134	7,813

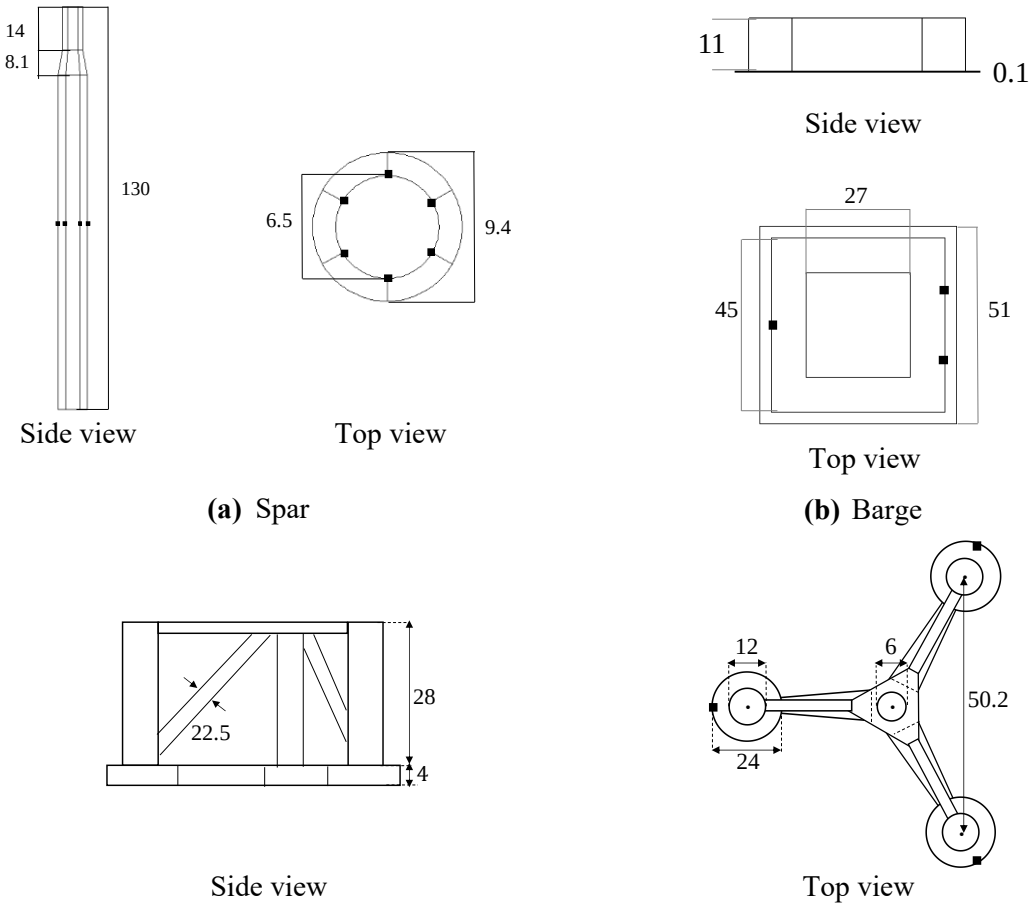

Figure 1. Overviewof three platform.

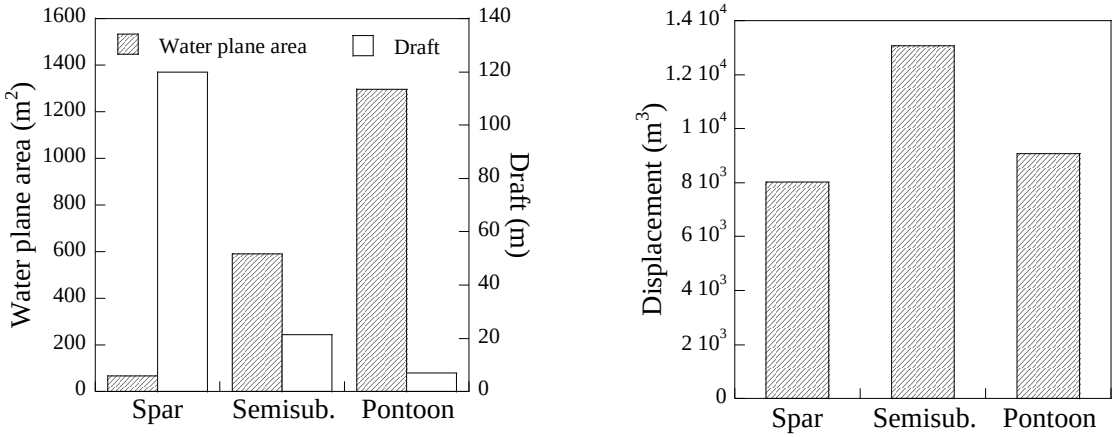

Figure 2. Comparison of water plane are, draft and displacement of three platforms.

The configuration of mooring lines is the same for three platform concepts. The number of mooring is six. The mooring angle is set as 40 degree in order to have the same mooring stiffness in the surge direction. Figure 3 shows the side and top views of mooring lines and Table 3 lists the main dimensions of mooring line. The water depth is set as 150 m.

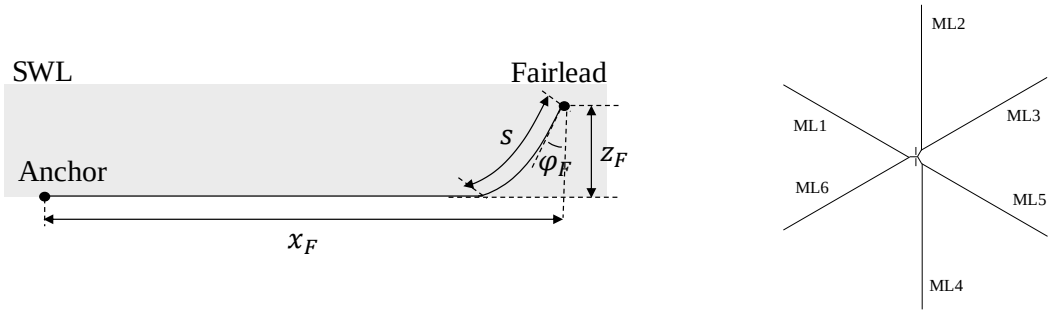

(a) Side view of one mooring line (b) Configuration of mooring lines

Figure 3. Side view and configuration of mooring line.

Table 3. Description of main dimensions of mooring line.

	Unit	Spar	Semisubmersible	Barge
Anchor radius	m	674.5	780	774.2(ML1,2), 777.3(ML3-6)
Anchor depth	m	-150	-150	-150
Radius of fairlead	m	5.2	36 / 36.7	22.5
Fairlead depth	m	-70	-13.3	-7
Unstretched line length	m	696.1	793	801.3
Line diameter	m	0.132	0.132	0.132
Mass per length in air	kg/m	382	382	382
Axial stiffness	N	2.42E+9	2.42E+9	2.42E+9

2.2. Hydrostatic restoring force

The platform concepts are categorized by the way of the floater stabilization in the pitch direction as mentioned by Butterfield et al. [8]. The static balance in the pitch direction is evaluated as the ratio of tower base moment into the restoring force of the platform. The linearized hydrostatic restoring force of the platform in the pitch direction C_{55} is calculated by the product of metacenter height $\overline{MG}$ and displacement volume as shown in Equations (1) and (2).

$$\overline{MG} = \frac{I_y}{V} - \overline{GC} \tag{1}$$

$$C_{55} = \overline{MG}\ \mathrm{V} \tag{2}$$

where I_y is the second moment of water plane area, V is the displacement volume, G is the center of gravity and C is the center of buoyancy. Figure 4 shows comparison of the parameters obtained from the static balance in the pitch direction for each platform. The metacenter height of spar is around 10 m due to the lower gravity center as described in Table 4. Barge has the highest metacenter since the second moment of water plane area is large. The hydrostatic restoring moment of barge is almost three times larger than that of spar.

Table 4. Description of main parameters of three platforms.

Item	Unit	Spar	Semisubmersible	Barge
Second moment of water plane area	m^4	88	146,942	297,400
Gravity center	m	-73	-11.09	-3
Buoyancy center	m	-62	-13.93	-3.5
Distance between gravity and buoyancy centers	m	10.7	-2.84	-0.5
Metacenter height	m	10.71	8.39	32.28
$-\overline{GC}$	m	10.7	-2.84	-0.5
I_y/V	m	0.01	11.23	32.78
Hydrostatic restoring moment	kN·m/rad	865,180	1,103,941	2,943,613

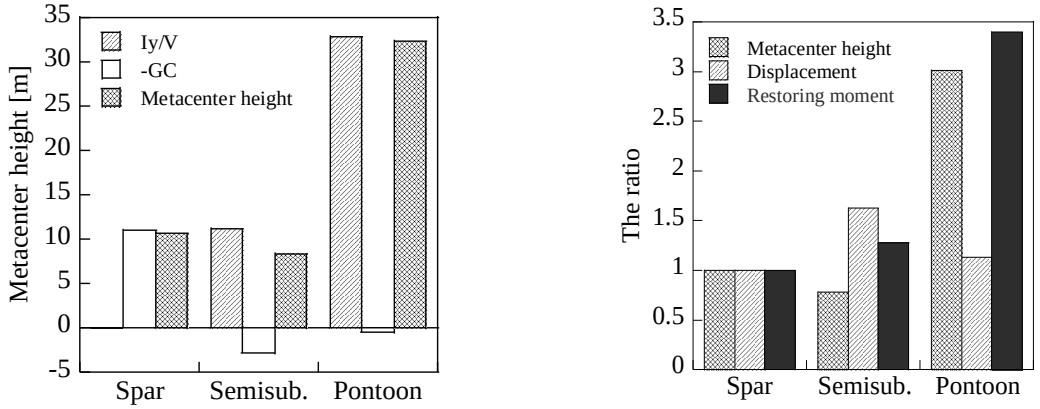

(a) Metacenter height (b) Hydrostatic restoring moment

Figure 4. The parameters obtained from the static balance in the pitch direction for each platform

.

2.3. Hydrodynamic force

The added mass, radiation damping and wave-excitation forces are obtained from the potential theory by using AQWA [17]. The drag forces are considered by applying Morison's equation.

Table 5 shows the drag coefficients used in this study. The drag coefficient of spar in the normal direction at high Reynolds number is 0.6. The drag coefficients of semisubmersible platform in the normal and axial directions are obtained from the forced oscillation test as shown by Ishihara and Zhang [18]. The drag coefficients of barge are also obtained by the forced oscillation test.

Figure 5 shows the comparison of added mass, radiation damping and Figure 6 illustrates the amplitude and phase of wave-excitation force (The sum of Froude Krylov and diffraction force) for each platform. The added masses of spar and semisubmersible platform are almost wave period independent, and that of barge depends on wave periods. Radiation damping in the heave direction shows much larger value in barge, comparing to the spar and semisubmersible platform due to the moonpool. The wave-excitation force for the barge in the heave direction shows much larger than spar and semisubmersible platform due to the larger water plane area. The barge has the opposite wave-excitation phase from the spar and semisubmersible platform in the pitch direction.

Table 5. Drag coefficients used for each platform.

Direction	Spar	Semisubmersible				Barge
Normal	0.6	Main column	0.56	Upper column	0.61	1.0
		Brace	0.63	Lower column	0.68	
Axial	None	9.6				5.0

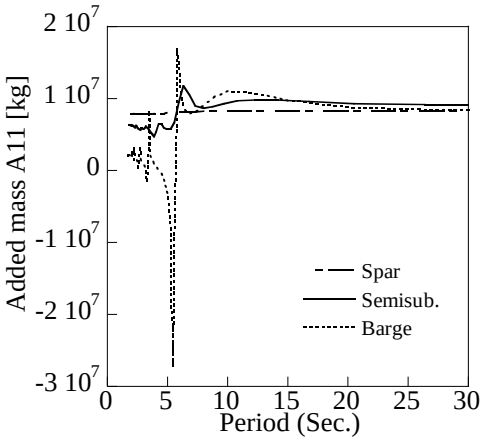

(a) Added mass in the surge direction

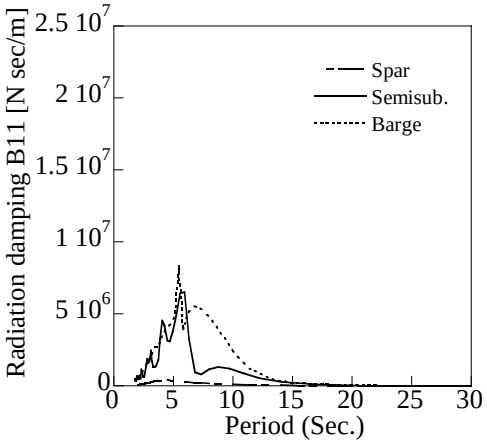

(b) Radiation damping in the surge direction

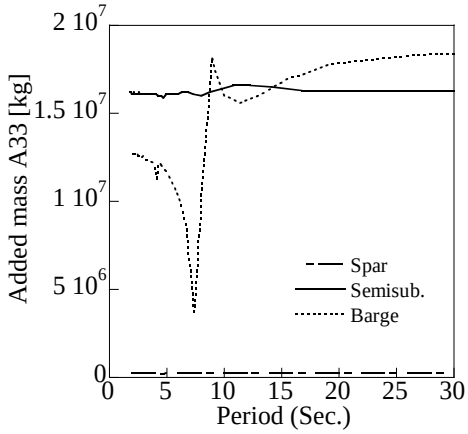

(c) Added mass in the heave direction

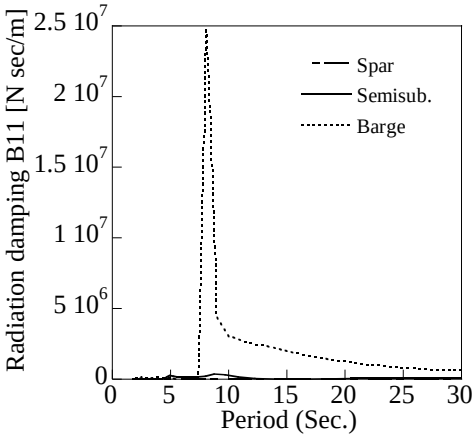

(d) Radiation damping in the heave direction

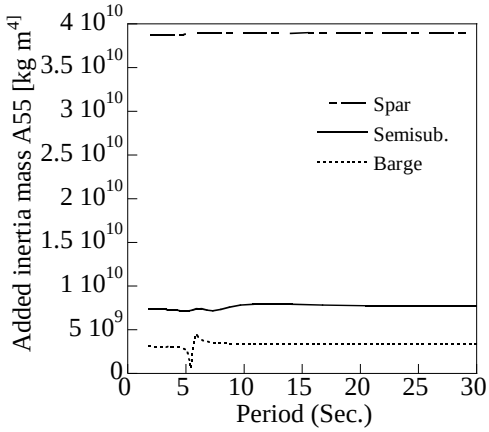

(e) Added inertia mass in the pitch direction

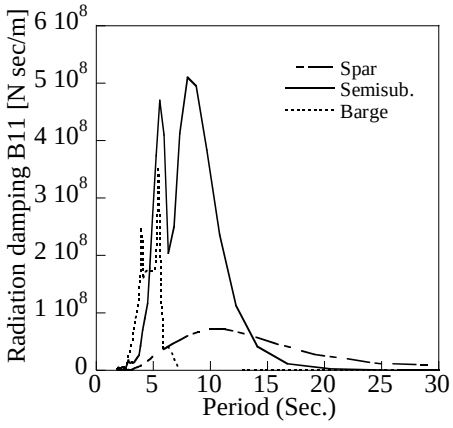

(f) Radiation damping in the pitch direction

Figure 5. Comparison of the linear hydrodynamic forces for each platform.

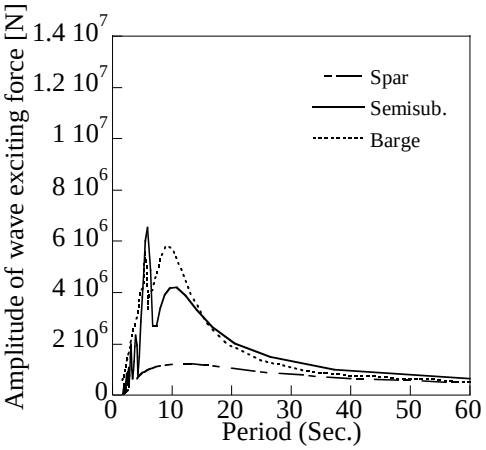

(a) Amplitude in the surge direction

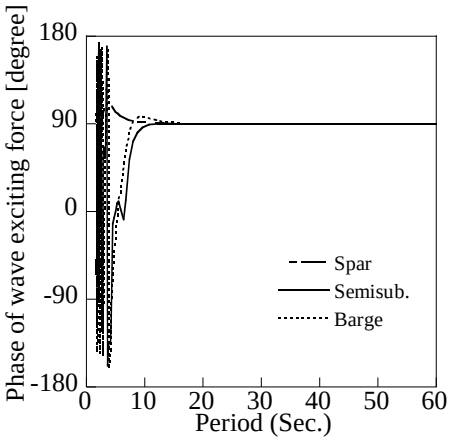

(b) Phase in the surge direction

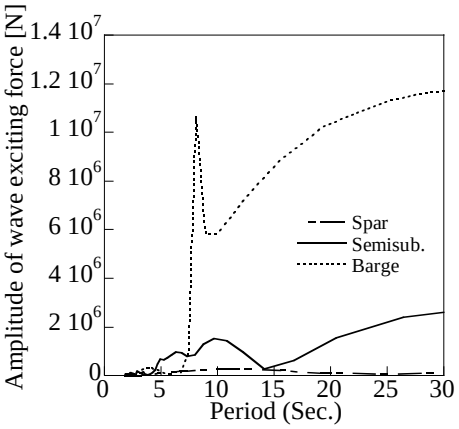

(c) Amplitude in the heave direction

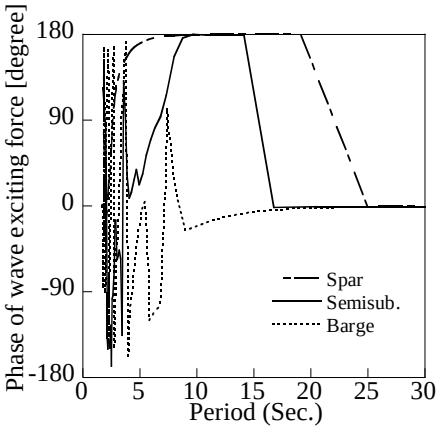

(d) Phase in the heave direction

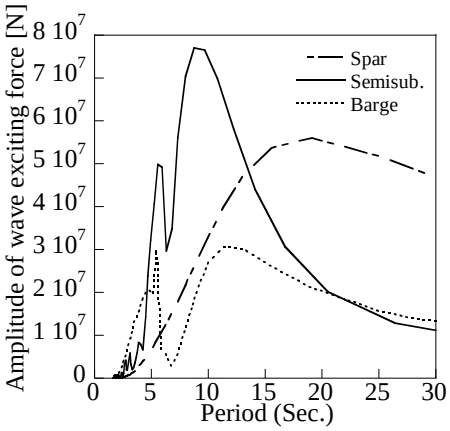

(e) Amplitude in the pitch direction

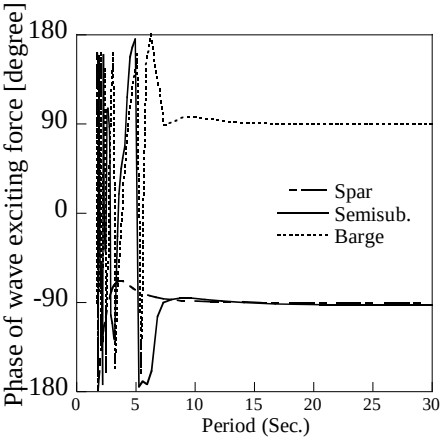

(f) Phase in the pitch direction

Figure 6. Comparison of the wave-excitation force for each platform.

3. Dynamic characteristics of three platform concepts

3.1. Natural period and Response Amplitude Operator

The dynamic analysis is performed to investigate dynamic characteristics of platforms by using FAST v8.10 [19]. Table 6 shows the predicted natural periods for each platform. The natural periods are also theoretically evaluated by Equation (3).

$$T = 2\pi\sqrt{\frac{M_{ii}+A_{ii}}{K_{ii}+C_{ii}}} \quad (3)$$

where M is the mass matrix of platform, A is the added mass matrix, C is the hydrostatic-restoring matrix from the water plane area and the center of buoyancy and K is the linearized hydrostatic restoring matrix from all mooring lines.

In order to investigate the difference of natural periods between three platforms, Figure 7 (a), (c) and (e) show the sum of mass and added mass normalized by the value of spar, which corresponds to the numerator in Equation (3). Figure 7 (b), (d) and (f) shows the sum of hydrostatic stiffness and mooring line stiffness normalized by value of spar, which corresponds to the denominator in Equation (3).

In the surge direction, the hydrostatic stiffness is almost zero and the mooring line stiffness shows almost the same value for all three platforms due to the same configuration of mooring line as shown in Figure 7 (b). The difference of natural periods among the three platforms is affected by the ratio of mass and added mass.

In the heave direction, the added mass of semisubmersible platform is much larger than the others. However, the hydrostatic restoring force of semisubmersible platform and that of barge are seven times and seventeen times larger than that of spar due to the difference of water plane area as shown in Figure 7 (d). The large hydrostatic force leads the shorter natural periods of the barge.

In the pitch direction, the hydrostatic stiffness significantly affects the natural periods. The hydrostatic stiffness of barge in the pitch direction is three times larger than that of spar as shown in Figure 7 (f).

Table 6. The predicted natural periods for each platform.

Direction	Natural periods (sec.)		
	Spar	Semisubmersible	Barge
Surge	67.2	78.6	64.9
Heave	27.6	17.2	6.7
Pitch	35.9	22.3	11.4

Response Amplitude Operators (RAOs) in the regular wave with the wave height of 2.5 m is predicted for each platform and those obtained from the water tank tests performed in the demonstration projects are used for validation.

Figure 8 reveals RAOs in the range of dominant wave periods. In the surge direction, motions for three platforms show almost the same value, while in the heave and pitch direction, the motion of barge is larger since the shorter natural period overlaps with the dominant wave periods.

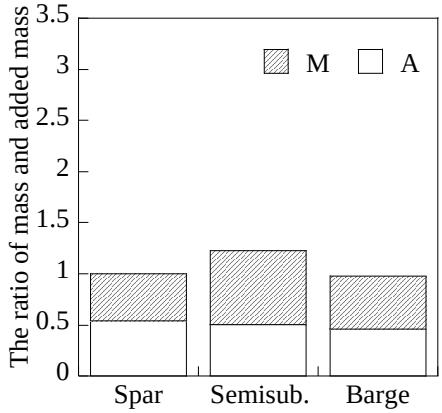

(a) Mass and added mass in the surge direction

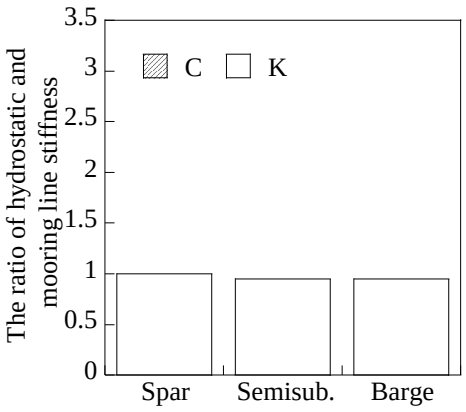

(b) Stiffness in the surge direction

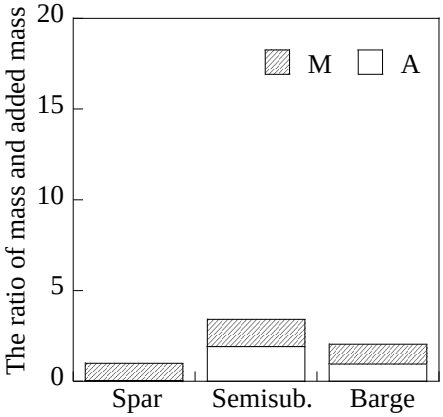

(c) Mass and added mass in the heave direction

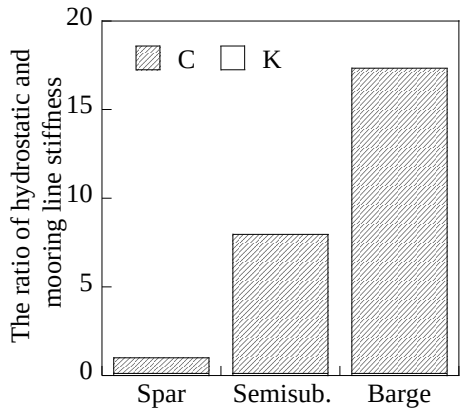

(d) Stiffness in the heave direction

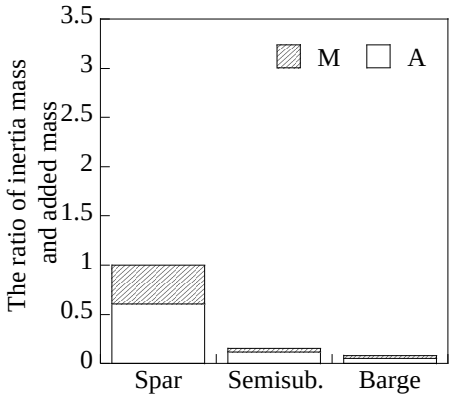

(e) Mass and added mass in the pitch direction

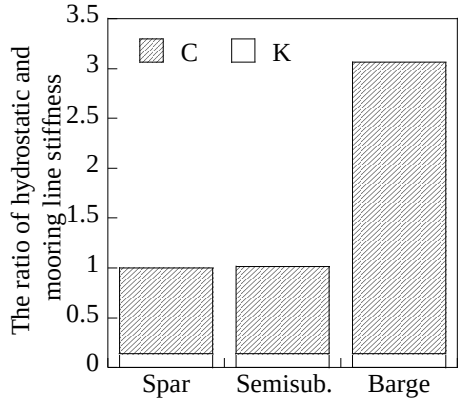

(f) Stiffness in the pitch direction

Figure 7. Comparison of mass, added mass, hydrodynamic stiffness and mooring line stiffness for each platform.

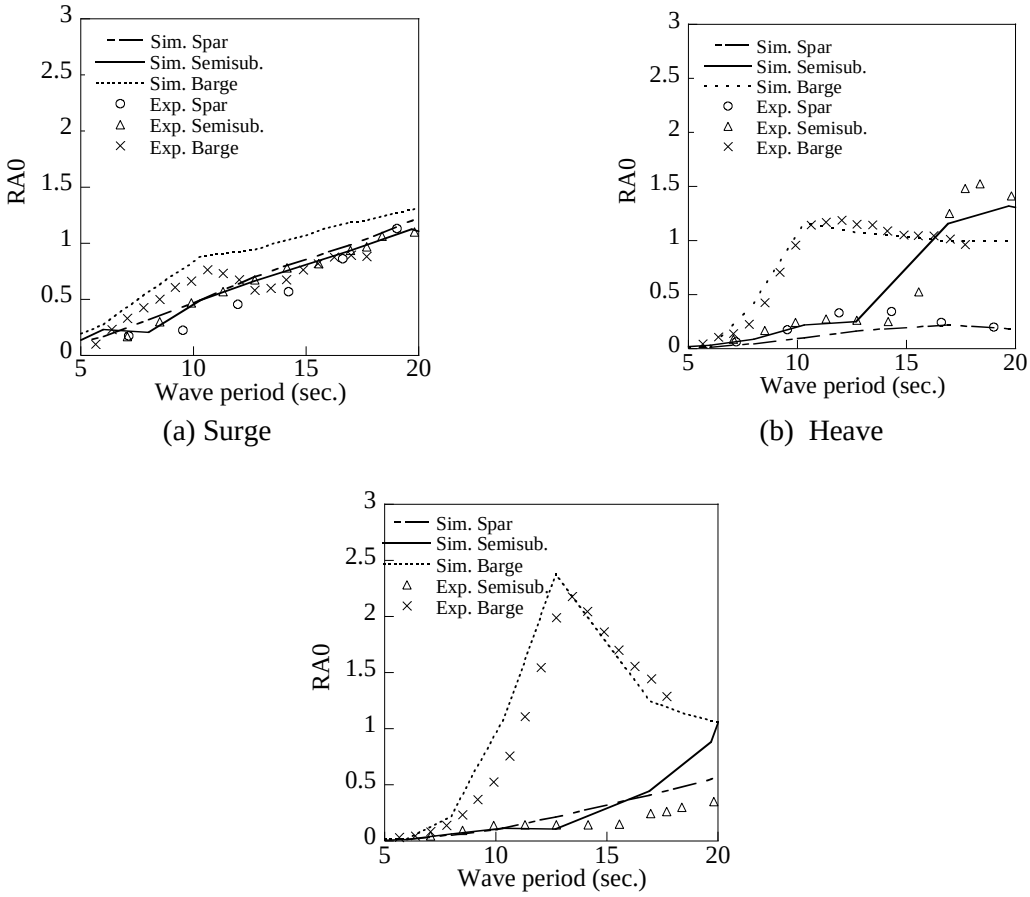

Figure 8. Comparison of RAOs in the surge, heave and pitch directions for each platform.

3.2. Maximum response for DLC6.1

DLC6.1 (Design Load Case 6.1) is calculated for the extreme condition in conformance with the requirement of IEC61400-3 standards [20]. In this study, the environmental conditions at Fukushima offshore site as shown by Ishihara et al. [21] is applied. The extreme wind speed of 50 m/s for the 50-year-recurrence period, turbulence intensity of 0.11, wind share of 0.11, wind direction of 0-degree, Kaimal spectrum are used for the wind conditions. The significant wave height of 11.7 m and the peak wave period of 14.76 second, the wave spectrum of Pierson-Moskowitz is applied for the wave conditions. The current speed is set as 1.44 m/s.

Figure 9 shows the floater motion and mooring force for each platform. In the surge direction, all three platforms show almost the same motion. In the heave and pitch directions, the barge shows the largest motion. Especially in the pitch direction, the motion of barge is around three times larger than the spar and semisubmersible platforms. The difference of mooring force is due to the difference of the fairlead depth.

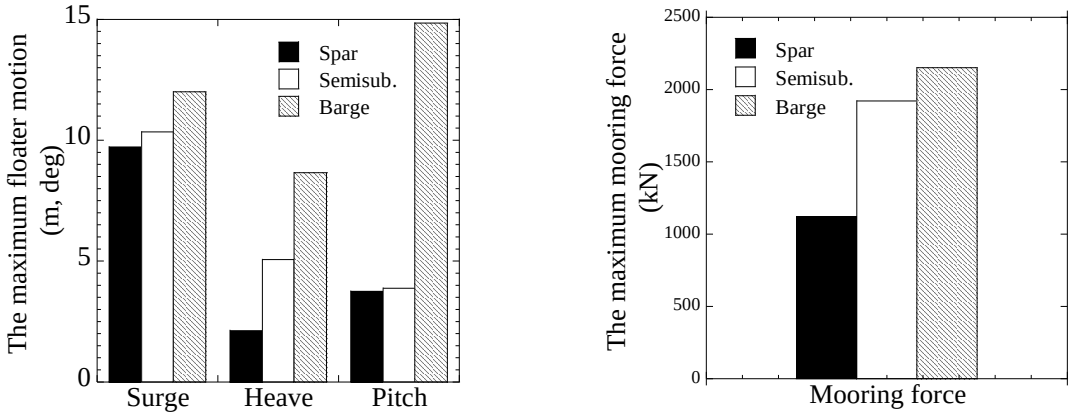

(a) Floater motion (b) Mooring force

Figure 9. Comparison of floater motion and mooring force for each platform.

4. Assessment of levelized cost of energy

The cost of each platform is estimated by using the engineering cost model. Figure 10 shows the steel weight of each platform, in which the ballast weight is excluded and the thickness is assumed based on the demonstration projects. The weight of semisubmersible platform is about twice that of spar. It should be noticed that the semisubmersible platform can be optimized by getting rid of the central column like WindFloat.

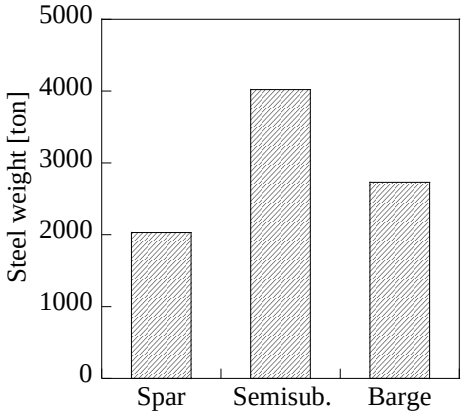

Figure 10. Steel weight of each platform.

For the barge, the tower bottom diameter and thickness need to be enlarged corresponding to the larger bending moment, which is not considered into the cost in this study. The installation steps are categorized into turbine assembly, floater towing and mooring installation. 0.92, 0.92, 3.69 €M per turbine are assumed for each step, and 0.6 k€/kW is assumed for the cable installation based on the next-generation demonstration project in Japan [5]. Operation and maintenance costs are also simply assumed as 0.1 €k/kW/year as shown in the reference [6] for the commercial phase, where 1 £ is converted to 1.11 €. Table 7 summarizes the assessed initial capital cost and O&M cost. 20-year-operation period, the interest rate of 3 %, capacity factor of 40 %, the availability of 90 % are assumed. The difference of LCOE is affected by the difference of steel weight for each platform. The optimized semisubmersible platform can reduce the LCOE.

Table 8 summarizes the characteristics in terms of cost for each platform. Spar is good for turbine, platform and mooring line, but needs the deep water in the port for installation. Semisubmersible platform is good for turbine, mooring line and installation, but the optimization of steel weight is a challenge. Barge is good for platform, mooring line and installation, but the turbine needs to allow a larger floater motion.

Table 7. Levelized cost of energy for each platform.

	Cost (€k/kW)		
	Spar	Semisubmersible	Barge
Design	0.1	0.1	0.1
Turbine	1.2	1.2	1.2
Platform	0.65	1.27	0.87
Mooring line	0.67	0.76	0.77
Cable	0.6	0.6	0.6
Installation	1.1	1.1	1.1
Initial Capital Cost	4.32	5.03	4.64
O&M	0.1	0.1	0.1
LCOE	12.38	13.89	13.06

Table 8. Summary of characteristics in terms of cost for each platform.

	Spar	Semisubmersible	Barge
Turbine	Good	Good	Challenge
Platform	Good	Challenge	Good
Mooring line	Good	Good	Good
Installation	Challenge	Good	Good

5. Conclusions

In this study, dynamic response and levelized cost of energy are compared among three type of platforms, namely, spar, semisubmersible and barge floating platforms. The conclusions are summarized as follows:

1) Three platforms are built based on the demonstration projects in Japan. The static characteristics on these platforms are quantitatively evaluated by the structural and stability parameters. The hydrostatic restoring moment of barge is almost three times larger than that of spar due to the large water plane area of barge platform.
2) The dynamic characteristic of three platforms are also evaluated. Shorter natural periods of barge in the heave and pitch directions leads the largest motion in the dominant wave periods. The maximum floater motion of barge in the pitch direction is almost three times larger than those of spar and semisubmersible platforms.
3) The levelized cost of energy for each platform is assessed by using the engineering cost model. The weight of semisubmersible is almost double larger than that of spar, which suggests the importance of optimization of the semisubmersible platform.

Acknowledgement

This research is carried out as a part of next-generation floating offshore project supported by National Energy Department Organization. Dr. Namba from the University of Tokyo supports dynamic analysis. Wind Energy Institute of Tokyo provides turbine models. The authors wish to express their deepest gratitude to the concerned parties for their assistance during this study.

References

[1] Equinor, The development of Hywind Scotland Pilot Park, https://www.equinor.com/en/what-we-do/hywind-where-the-wind-takes-us.html
[2] T. Utsunomiya, I. Sato, T. Shiraishi, E. Inui, S. Ishida, Floating offshore wind turbine demonstration project at Goto islands, Japan, OCEANS 2014 – TAIPEI, pp. 1-7, 2014
[3] WindFloat, http://www.principlepowerinc.com/en/windfloat
[4] Fukushima Offshore Wind Consortium, Fukushima Floating Offshore Wind Farm Demonstration Projects, http://www.fukushima-forward.jp/english/
[5] Next generation floating offshore wind power generation system demonstration research (barge type), https://g-local.co.jp/works/barge/
[6] The carbon trust, Floating offshore wind: market and technology review, 2015. https://www.carbontrust.com/media/670664/floating-offshore-wind-market-technology-review.pdf
[7] J. V. Taboada, Comparative analysis review on floating offshore wind foundation, 54th Naval Engineering and Maritime Industry Congress in Ferrol, 2015. https://sectormaritimo.es/comparative-analysis-review-on-floating-offshore-wind-foundations-fowf
[8] S. Butterfield, W. Musial, J. Jonkman, P. Sclavounos, L. Wayman, Engineering challenges for floating offshore wind turbines. Copenhagen Offshore Wind 2005 Conference and Expdition Proceedings, 26-28 October, Copenhagen, 2005. https://www.nrel.gov/docs/fy07osti/38776.pdf
[9] J. Cruz , M. Atcheson (Eds.), Floating offshore wind energy, Green Energy and Technology, Springer, 2016.
[10] J. M. Jonkman, D. Matha, Dynamics of offshore floating wind turbines-analysis of three concepts, Wind Energy 14, 557-569, 2011.
[11] B. J. Koo, A. J. Gouppe, R. W. Kimball, K. F. Lambrakos, Model tests for a floating wind turbine on three different floaters, J. Offshore Mech, Arct. Eng 136(2), 020907, 2014.
[12] A. J. Goupee, B. J. Koo, R. W. Kimball, K. F. Lambrakos, H. J. Dagher, Experimental comparison of three floating wind turbine concepts, J. Offshore Mech. Arct. Eng 136(2), 020906, 2014.
[13] H. Bagbanci, D. Karmakar and C. G. Soares, Comparison of spar and semisubmersible floater concepts of offshore wind turbines using long-term analysis, J. Offshore Mech. Arct. Eng 137(6), 061601, 2015.
[14] D. Roddier, A. Peiffer, A. Aubault and J. Weinstein, A generic 5 MW wind float for numericfal tool validation and comparison against a generic spar, ASME Paper No. OMAE 2011-50278. 2011.
[15] A. Myhr, C. Bjerkseter, A. A. Gotnes, T. A. Nygaard, Levelized cost of energy for offshore floating wind turbines in a life cycle perspective, Renewable Energy, 66, 714–28, 2014.
[16] Jonkman J M, Dynamic modelling and loads analysis of an offshore floating wind turbine, *Technical Report NREL/TP-500-41958*, 2007. https://www.nrel.gov/docs/fy08osti/41958.pdf
[17] AQWA, Versio 15.0, ANSYS. Inc, 2013.
[18] T. Ishihara, S. Zhang, Prediction of dynamic reponse of semisubmersible floating offshore wind turbine using augmented Morison's equation with frequency dependent hydrodynamic coefficients, Renewable Energy, 131, 1186-1207, 2019.
[19] FAST v8.10. https://nwtc.nrel.gov/FAST8.
[20] International Electrotechnical Committee IEC 61400-3-1, Wind energy generation systems - Part 3-1: Design requirements for fixed offshore wind turbines, 2019.
[21] T. Ishihara, K. Shimada and A. Imakita, Metocean design condition for Fukushima FORWARD Project, Proc. Int. Conf. of Grand Renewable Energy ,Yokohama, Japan, 2014.